energies

MDPI

Article

Evaluation of Hydrogen Yield Evolution in Gaseous Fraction and Biochar Structure Resulting from Walnut Shells Pyrolysis

Elena David

National Research and Development Institute for Cryogenics and Isotopic Technologies—ICSI Rm. Valcea, Street Uzinei, No.4, 240050 Rm. Valcea, Romania; elenadavid2004@yahoo.com or Elena.David@icsi.ro

Received: 3 November 2020; Accepted: 30 November 2020; Published: 2 December 2020

Abstract: Conversion experiments of wet and dry walnut shells were performed, the influence of moisture content on the hydrogen yield in the gas fraction was estimated and the resulted biochar structure was presented. Measurements of the biochar structures were performed using X-ray diffraction and scanning electron microscopy methods. The results demonstrate that heating rate played a key role in the pyrolysis process and influenced the biochar structure. Under fast heating rate, the interactions between the water vapors released and other intermediate products, such as biochar was enhanced and consequently more hydrogen was generated. It could also be observed that both biochar samples, obtained from wet and dry walnut shells, had an approximately smooth surface and are different from the rough surface of the raw walnut shell, but there are not obvious differences in shape and pores structure between the two biochar samples. The increasing of the biochar surface area versus pyrolysis temperature is due tothe formation of micropores in structure. The biochar shows a surface morphology in the form of particles with rough, compact and porous structure. In addition the biochar structure confirmed that directly pyrolysis of wet walnut shells without predried treatment has enhanced the hydrogen content in the gas fraction.

Keywords: walnut shell; moisture content; pyrolysis; gas fraction; H_2 yield; biochar structure

1. Introduction

The main organic components in biomass (i.e., including agricultural residue) and their chemical structure have a substantial role in improving of the processes used to produce fuels and chemicals [1–3]. The lignocellulose from biomass contains four major components and these are: cellulose, hemicellulose, lignin and extractives [3]. The first three types of components have large molecular weights and constitute the main mass of biomass, while the extractives are compounds of smaller molecular size, and are in a low amount [4,5]. Hydrogen can be obtained by biomass pyrolysis and gasification but these technologies need further improvement and development [6–8].Hydrogen production from biomass brings some advantages [9] such as reducing the cost to oil imports, a level of stable price and the balance of CO_2 is stabilized by ≈25–30% [10].

The H_2 production from different biomass sources is based on thermochemical and biological processes. The thermochemical process has a higher efficiency ($\eta \approx 50\%$) and the cost is low [11,12].

Thermocatalytic biomass conversion includes pyrolysis, gasification and reforming processes while the biological route refers to the fermentative process [13–16]. These conversion processes produce gases such as, H_2, CO_2, CO, CH_4 and also light gaseous hydrocarbon. The use of catalyst processes together with separation techniques could help to increase the yield of hydrogen in the gaseous fraction [17]. The mixture of H_2 and CO, known as syngas, could be used as an intermediate for the obtaining of gasoline by Fischer–Tropsch synthesis [15,16]. Although, research has been focused on

how the different conversion processes could be improved to increase the productivity, there is also high attention on the environmental impact of using the different technical routes for hydrogen-rich syngas production [14,17]. There are extensive review studies on hydrogen production by CH_4conversion, agricultural residues by fermentation process [18], photochemical conversion of hydrogen sulfide and thermochemical biomass conversion [19–21]. None of these reviews referred to the production of hydrogen-rich gas by thermal biomass conversion using their own moisture content.

At temperatures in the range of 500–800 °C, the biomass suffers a thermal degradation and results in a liquid and gaseous fraction that usually contains bio-oil product and CO, H_2, CO_2, CH_4, H_2O and other hydrocarbons (C_2–C_7) as gases [11].Composition of gaseous product resulted from the biomass gasification depends on the type of reactor, gasifying agent and the feedstock composition [22–24]. The conversion of biomass is generally given by the reaction:

$$\text{Biomass} + \text{heat} + \text{gasifying agent (air, steam)} \rightarrow CO, CO_2, H_2O, H_2, CH_4 + C_{2-7} + \text{tar} + \text{char} + \text{ash} \quad (1)$$

In a pyrolysis process of the biomass, the first step is a thermochemical degradation of the main components (cellulose, hemicellulose and lignin) and results in biochar, liquid (tar) and volatiles [4,25,26]. Further, the biochar and tar gasification reactions could appear and other equilibrium reactions to take place. Figure 1 shows the possible products resulted from a pyrolysis process. During the biomass conversion together with the gaseous phase, it formed tar and its separation and removing is difficult to be achieved using only a physical method [27]. The products distribution and the composition of gaseous fraction depend on some important parameters, such as conversion temperature, the raw biomass used and the type of reactor [28]. The gasification process ensures the possibility to convert biomass feedstock into clean gas fuel/synthesis gas [29,30]. The synthesis gas is mainly formed of H_2 and CO, and it is known as bio-syngas if is obtained from biomass [4]. Bio-syngas can be obtained from biomass by catalytic and non-catalytic processes, and also using a gasification agent (air/steam/CO_2) [31].

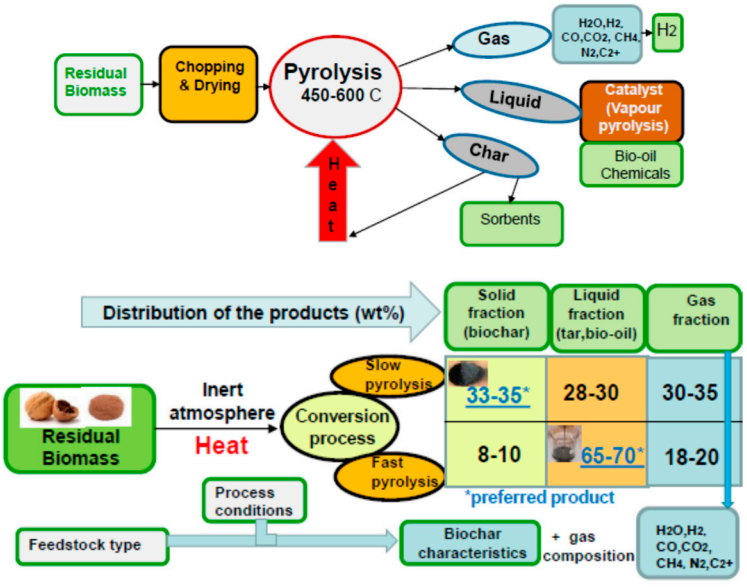

Figure 1. Possible products resulted from a pyrolysis process and the distribution of products.

The biomass conversion using steam as a gasification agent is a promising way used for production of gas with high H_2 content [25]. In recent years, H_2 production by biomass pyrolysis and/or gasification became a subject intensively researched in the domain of biomass utilization [32]. Previous studies [33,34] have reported that the introduction of steam during biomass conversion process lead to an increasing of H_2 amount due to the tar and higher molecular weight hydrocarbons

reforming, and the water gas shift reaction [2,5,6].Using steam as an oxidizer, the following chemical reaction can be written:

$$CH_{1.31}\,O_{0.69} + 1.31\,H_2O \rightarrow 1.97\,H_2 + CO_2 \quad (2)$$

with the biomass chemical formula, which was calculated using elemental analysis, Table 1.

Table 1. Proximate ultimate analyses and of walnut shells.

Chemical Element	Ultimate Analysis (wt.%)	Proximate Analysis (wt.%)	
C	49.26	Fixed carbon	10.76
H	5.38	Moisture	7.85
O	45.08	Volatiles	80.21
N	0.28	Ash	1.18
H/C	1.3105	Cellulose	34.26
O/C	0.6863	Hemicellulose	27.74
N/C	0.0048	Lignin	36.45

According to reaction (2), a minimum water (steam)/biomass (S/B) ratio of 0.968 is established for the theoretical maximum H_2 yield. The recent studies refer to modification of the operating parameters, the use of different types of reactors and catalytic processes, etc. [32–34]. Unfortunately, no studies have been performed related to the reduction of costs due to the way the steam is supplied [35] even if this consumes a big quantity of energy from the whole process. Usually, the raw biomass contains a big fraction of moisture, which even exceeds 40–50 wt.% (wet basis). In the conventional biomass steam gasification (CBSG), own moisture from biomass is removed before conversion by a predrying step and then the predried biomass is subjected to the gasification/pyrolysis process [36–39]. The steam used as a gasification agent is usually provided by an auxiliary source such as a generator or boiler. Both the predrying step and steam supply need energy consumption and for this reason the CBSG process is expensive and complex. Considering these aspects, in this work a method of H_2 rich gas production by agricultural residue pyrolysis in an autogenerated moisture atmosphere was experimented. In this method, the agricultural residue, including walnut shells, with high moisture content was used as starting raw materials for a pyrolysis reactor. Walnut shells were used because it is a biomass residue that results in large quantities in the geographical area, contains high moisture content and is not valorized The method has used its own moisture from the initial biomass sample as a reactant to combine with the intermediate products resulted from the pyrolysis and in this way to produce additional gas (hydrogen). Additionally, to obtain some basic useful information, the influence of several parameters such as pyrolysis reactor temperature, heating rate, moisture content in the agricultural residue samples and stripping gas flow on the efficiency of the pyrolysis process was investigated and evaluated. The characteristics of the resulted biochar by the pyrolysis process were also presented.

2. Experimental Part

2.1. Materials and Sample Preparation

In this study, the residual biomass, including walnut shells (WSs), was employed as raw materials. The raw walnut shells in hemispherical shape with about 25–35 mm diameter and 2–3 mm thickness were supplied by the Research Station for Fruit Growing Valcea (Figure 2). The walnut shells were collected from the hill area of Valcea county, approximately 35 km away from the town of Rm. Valcea (located on the parallel 45°06′ N).

(**a**) (**b**)

Figure 2. Raw agricultural residue: (**a**) walnut shell in hemispherical shape and (**b**) walnut shell powder.

Table 1 shows the composition and elemental analysis for walnut shells.

Walnut shells were first crushed, then grinded and sieved to obtain particle size ≤ 1 mm. The proximate analysis of raw walnut shells was done according to ASTM D3174-04 for ash analysis and ASTMD3175-89a for volatile matter. The ultimate analysis to determine the quantity of C, H and N (O calculated from the difference) was made according to ASTM D5291-96 using a FLASH-2000 Elemental Analyzer (Table 1). The scanning electron micrograph (SEM) analysis of the raw walnut shells and biochar samples obtained after pyrolysis was performed by using Jeol JSM-6060.

All chemicals used in this study were of analytical grade. To study the effect of moisture content, the walnut shells were dried naturally, by sun drying to different moisture contents: (a) wet walnut shell sample (WS_W), the as-received walnut shell, with a moisture content of ≈48.15 w.% (wet basis); (b) a partially predried fraction of the as received wet walnut shell sample (WS_{PD}), with a moisture content of ≈33.68 wt.% (wet basis) and (c) totally predried walnut shell sample (WS_{TD}) with a moisture content of ≈7.85 wt.% (wet basis).The moisture content was determined according to ASTM D4442-07.

A measurement of specific surface area of the biochar samples has been performed by N_2 adsorption at −196.15 °C, using a surface analyzer (Quantachrome Instruments, Corporate Headquarters USA). The total volume of the pore (Vt) was determined from the quantity of N_2 vapor adsorbed at relative pressure of 0.95. The total surface area (St) was determined using BET equation in the relative pressure range 0.05–0.35. The limits between micro- and mesopores and also meso- and macropores were taken following the IUPAC nomenclature and the Barrett–Joyner–Halenda (BJH) method was used to establish the mesopore size distribution. XRD analysis was performed using D/max-2200/PC, Rigaku, Japan, and copper KR radiation (40 kV, 20 mA) as the X-ray source. Scanning electron microscopy (SEM) was performed using a microscope JSM-7500 F (JOEL-Japan), operated at 10 kV.

2.2. Experimental Pyrolysis Tests

Two types of reactors were used for the pyrolysis experimental tests, one was a stainless steel reactor, used for the slow pyrolysis tests and another one was a quartz tube reactor, used for the fast pyrolysis tests, each depending on the process parameters required. Figure 3a–c shows a schematic diagram of the experimental system and the dimensions for the stainless steel reactor and quartz reactor.

The experimental system consisted of four parts: (I) the stainless steel reactor, (II) the quartz tube reactor, (III) the gas clean and collection system and (IV) the temperature control system. Slow pyrolysis tests were carried out in the stainless steel reactor (4). The walnut shell sample (100 g, air-dry basis) was placed in the reactor (350 mm length × 25.4 mm i.d.). Next, the reactor was stripped with the inert gas (N_2) for 5–10 min. The experiments were started by heating the reactor at a temperature in the range of 300–800 °C, at a heating rate of 5 °C/min, using electric furnace of 1100 °C. For temperature value comparison, the temperatures in the middle of the biomass bed and of the reactor wall were measured using two thermocouples, respectively. The volatile products were continuously removed from the reactor by stripping with N_2 gas. The volatile products were passed through the two coolers and then by a glass wool filter to remove the impurities from the volatile products, as shown in Figure 3. The gas fraction was stored into a gas tank, and the volume was determined with a wet gas-meter. After the reactor temperature was reached, the reactor was maintained for 20 min at that temperature, after which the heating was interrupted and the reactor was naturally cooled.

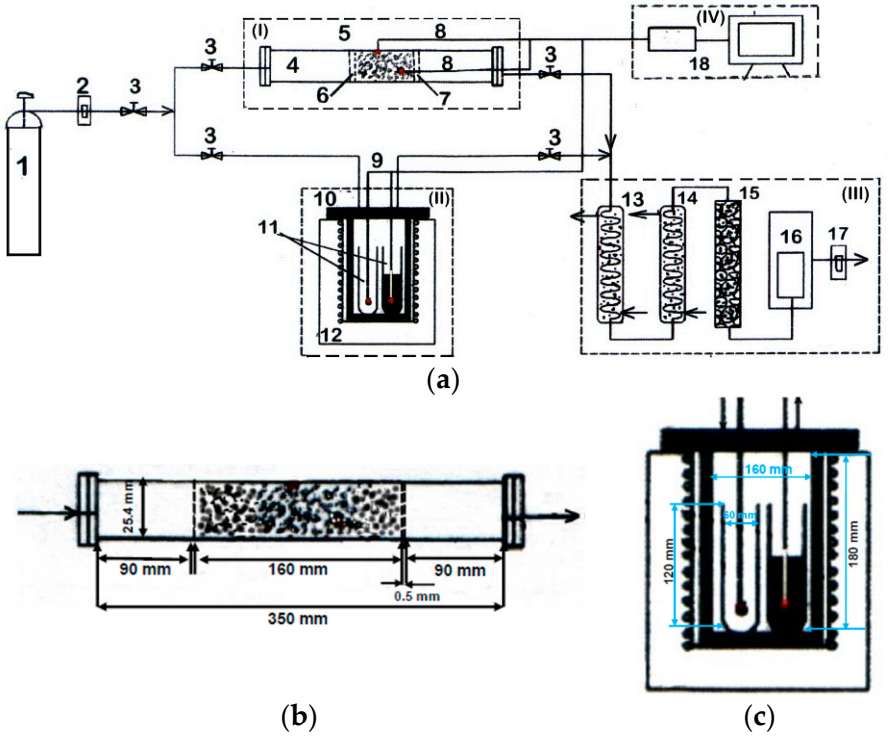

Figure 3. (**a**)—Schematic diagram of the experimental system: (1) N_2 tank, (2) N_2 gas flow-meter, (3) valve, (4) stainless steel reactor; (5) electric tube furnace; (6,7)grate; (8, 9) thermocouples; (10) stainless steel reactor; (11) quartz tube; (12) electric furnace; (13,14) cooler; (15) filter with glass wool; (16) gas tank; (17) pressure gauge with gas flow-meter; (18)data acquisition unit; (**b**)—stainless steel reactor-position (4) from the scheme; (**c**)—quartz tube reactor-part (II) from the scheme.

Fast pyrolysis tests were performed using the reactor made of quartz. To obtain a fast heating rate, the amount of used biomass was only 10 g (air-dry basis). Next, a ceramic boat containing biomass sample was put into the reactor (120 mm length × 60 mm i.d), the reactor was stripped with the inert gas (N_2) for 5–10 min and then was heated in a N_2 atmosphere using an electric furnace, until the desired temperature (the range of 500–800 °C) at a heating rate of 50 °C/min, and held for 20 min, then the heating was interrupted. The gas was cleaned and then collected in the same way as that in the slow pyrolysis tests. The composition of the gaseous phase (H_2, CH_4, CO and CO_2), was established using a gas chromatograph type Varian CP-3800 with TCD and FID detectors, equipped with three columns: (i) a 5 Å molecular sieve column,(ii) a Porapak N column and (iii) a Chromosorb column, and using argon as carrier gas. The amount of biochar was determined by weighing with an analytical balance having a precision of ±0.1 mg.

The carbon conversion quantifies the efficiency of the pyrolysis process. The carbon conversion efficiency (η_{cc}) was established in terms of the moles of carbon in the walnut shells that are transformed to carbon containing gases [36], in accordance with Equation (3):

$$\eta_{cc} = [M_{product}/M_{biomass}] \times 100 \quad (3)$$

where $M_{product}$ represent the carbon moles in gas fraction (CO, CO_2 and CH_4), and $M_{biomass}$ represent the carbon moles in the walnut shell sample.

3. Results and Discussion

3.1. The Effect of Reactor Temperature on the Pyrolysis Process

It is known that temperature plays a very important role in the biomass conversion (pyrolysis/gasification) process. In the present study, the reactor temperature was varied in the range of 300–800 °C with a step of 100 °C. The reactor temperature and the obtained results are shown in Figures 4 and 5.

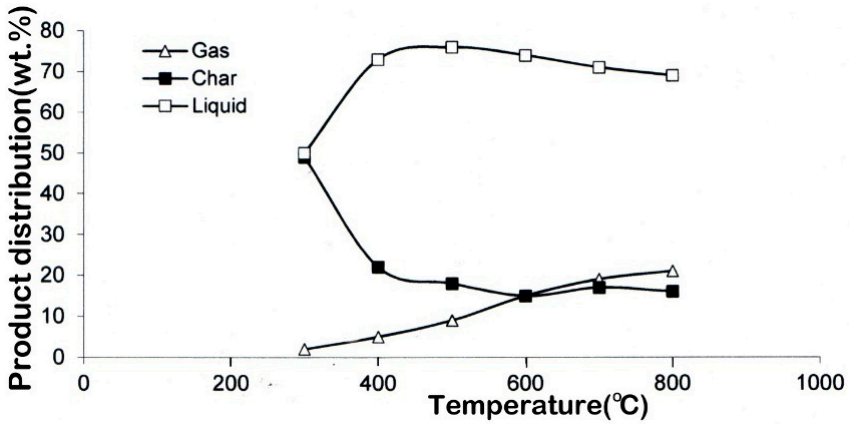

Figure 4. Temperature effect on product distributions (slow pyrolysis; moisture content, 48.15 wt.%; stripping gas flow rate, 40 L/h).

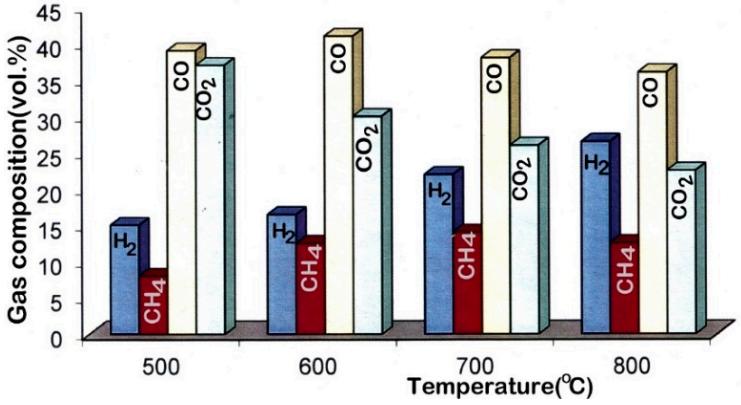

Figure 5. Temperature influence on gas composition (slow pyrolysis; moisture content, 48.15 wt.%; striping gas flow rate, 40 L/h).

As can be observed in Figure 4, the gas yield increased with the reactor temperature, while the biochar yield decreased. This behavior was due to the cracking reactions as a result of the temperature increasing into the reactor, the consequence was that more gas was produced. The tar yield increased first and then decreased, and a maximum of 76.18 wt.% appeared in the range of 500–600 °C, this temperature value indicating a suitable one for liquid fraction production (water and tar). These results are similar to the previous research [37,38], which used predried biomass. In addition, it was found that 86.05 wt.% of walnut shells put into the reactor was converted in volatile products (gas, tar and water) at 500 °C, and this percent increased slightly with the temperature from a reactor, being 87.08 wt.% at 800 °C. These results show that an important part of the volatile products were released from the biomass sample before 600 °C, and after that, the increasing of the temperature had a little effect on the walnut shells decomposition.

It should be noted that the liquid fraction yield was high in the all ranges of temperature analyzed. At 800 °C, the yield of liquid fraction even reached ≈68.9 wt.%. Such a high liquid yield indicated that the reactions between the intermediate components (volatile and char) and the generated water vapors were limited, possibly due to the low heating rate and also due to the presence of stripping gas. These results are in agreement with data presented in the literature [34,35]. In Figure 5 the effect of the temperature on gas product compositions shown. As can be seen, with the increasing of the temperature, the amounts of H_2 and CH_4 increased from 15.68 to 27.02 vol.% and from 8.57 to 13.37 vol.%, respectively. CO amount had a smaller decreasing from 39.36 to 36.71 vol.% between 500 and 800 °C, while CO_2 content decreased from 48.85 to 23.04 vol.% with the temperature increasing. The increasing of the gas yield and the H_2 content indicates that the H_2 yield increased with the temperature and this can be attributed to the cracking reactions and steam reforming process at a higher temperature to form much more H_2 [35,37].

3.2. The Effect of Moisture Content on Hydrogen Yield

In this study, walnut shell samples with different moisture contents (WS_W, WS_{PD} and WS_{TD}) were tested in the pyrolysis process. For this, two types of reactor were used, to provide different heating rates. Figure 6 presents the influence of the humidity on the hydrogen yield. The gas yield and the conversion efficiency of the biochar and the gas composition for each experimental test including CO, H_2, CO_2 and CH_4 are shown in Figure 6 and Table 2. The pyrolysis of WS_W and WS_{PD} samples represents the biomass pyrolysis process in which the wet and predried biomass were used as initial raw materials. In comparison with the WS_{TD} sample pyrolysis, it was found that the hydrogen yield increased with the increasing of the humidity content, this indicating that a direct pyrolysis of the wet biomass sample without a predrying treatment had favored an increasing of hydrogen production. This could be justified by that the water vapors released from the humidity of the wet walnut shells sample would react with the intermediate compounds such as volatile and biochar, to for much more H_2.

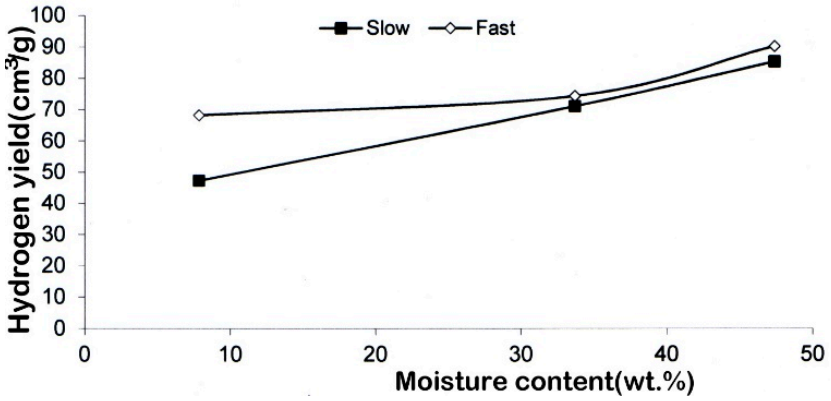

Figure 6. Effect of the moisture content on hydrogen yield under the slow and fast pyrolysis process.

In addition, with the increasing of the humidity content, the water vapors partial pressure increased and thus it improved hydrogen yield. The main reactions that took place during the pyrolysis of wet biomass sample could be as follows:

Drying process:

$$\text{Wet Biomass} + \text{Heat} \rightarrow \text{Water Vapors} + \text{Dry Biomass} \quad (4)$$

Generally, the hydrocarbons reforming reaction can be written as:

$$C_nH_m + 2nH_2O \rightarrow nCO_2 + [2n + (m/2)]H_2 \quad (5)$$

The reforming reactions of methane:

$$CH_4 + H_2O = CO + 3H_2\ \Delta H^\circ_{298} = 206\ \text{kJ/mol}. \quad (6)$$

$$CH_4 + 2H_2O = CO_2 + 4H_2\ \Delta H^\circ_{298} = 165\ \text{kJ/mol}. \quad (7)$$

The water gas shift reaction:

$$CO + H_2O \rightarrow CO_2 + H_2\ \Delta H^\circ_{298} = 41.5\ \text{kJ/mol}. \quad (8)$$

As can be seen in Figure 6 and Table 2, under slow pyrolysis conditions, the hydrogen yield and amount increased, while the gas yield and the efficiency (η) showed little variations with the moisture content from the biomass sample. However, under fast pyrolysis conditions, these variables increased more. With the increase of the moisture content from 7.85% to 48.15%, the hydrogen yield increased. The results obtained are similar to other studies [17,19,36]. Since this study investigated the evolution of hydrogen content in the gas fraction obtained, Table 2 shows the standard deviation from the determined average value (each average value representing the arithmetic average of at least three tests), and the dispersion. It can be seen that the standard deviation for the samples with the highest moisture content (48.15 wt.%) was ±0.2455 for slow pyrolysis and ±0.0086 for fast pyrolysis (the standard deviation was much smaller in the case of the fast pyrolysis process).

Table 2. The influence of the moisture content on the gas yield, conversion efficiency (η) and gas composition (40 L/h striping gas flow rate) and statistical processing of experimental data obtained for the hydrogen content in the gas fraction, depending on the moisture content of the walnut shells samples.

Parameter	Sample					
	Slow Pyrolysis			Fast Pyrolysis		
	WS_W	WS_{PD}	WS_{TD}	WS_W	WS_{PD}	WS_{TD}
[a] Moisture content (wt.%)	48.15	33.68	7.85	48.15	33.68	7.85
Heating rate (°C/min)	5	5	5	50	50	50
Temperature pyrolysis (°C)	700	700	700	700	700	700
Stripping gas flow rate (L/h)	40	40	40	40	40	40
[b] Gas yield(cm^3/g)	322	325	335	419	489	540
η (vol.%)	26.74	27.29	27.58	49.65	45.61	40.68
Gas composition (vol.%)						
H_2	26.86	23.02	21.69	15.77	14.72	11.23
CO	36.58	37.75	37.42	42.37	41.62	39.18
CO_2	23.04	25.13	26.46	31.46	33.52	39.22
CH_4	13.52	14.10	14.43	10.40	10.14	10.37
Statistical analysis						
Medium value (x_m)	26.86	23.02	21.69	15.77	14.72	11.23
Standard deviation (s)	±0.2455	±0.0458	±0.0774	±0.0086	±0.1317	±0.0361
Dispersion (s^2)	0.0602	0.0021	0.0059	0.0007	0.0173	0.0013

[a] Determined on the wet basis; [b] Determined on the dry ash free basis.

Comparing the results from both the slow and the fast pyrolysis, it could be observed that under fast pyrolysis conditions the influence of the moisture content on the pyrolysis process was stronger than that under slow pyrolysis conditions. This may be related with the interactions that take place between the generated water vapors and the intermediate compounds, such as volatile and biochar, produced from different heating rates. For the slow pyrolysis conditions, the water vapors generated, from moisture content, was not totally removed by striping gas before coming in contact with the intermediate compounds, due to the long time of drying and pyrolysis, thus, determining a poorer influence of moisture content on the subsequent pyrolysis process.

In the case of the fast pyrolysis process, however, both the moisture evaporation and intermediate products generation (volatile and biochar) occur in a shorter time, which lead to improving the interactions between water vapors–volatile and the water vapors–biochar.

Figure 7 shows the temperature curves of different WS samples during pyrolysis tests using the two types of reactors.

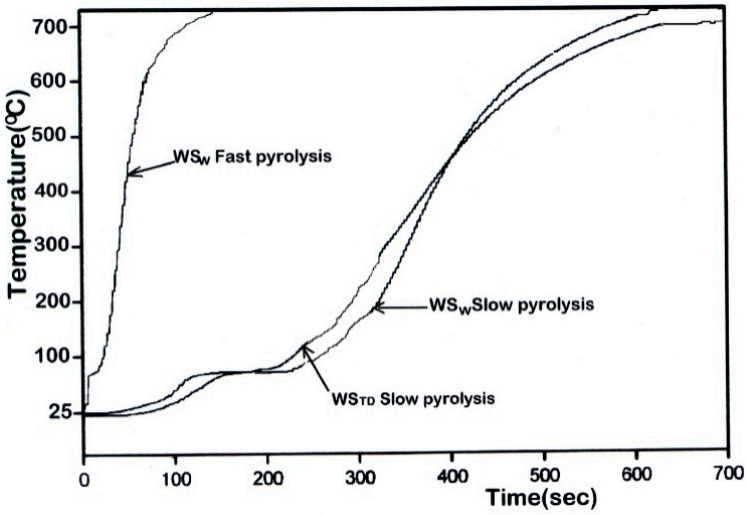

Figure 7. Temperature curves of different walnut shell (WS) samples during pyrolysis tests using the two types of reactors.

The temperature profiles show that the time duration of both drying and pyrolysis processes was reduced when the heating rate increased. Consequently, the direct use of the wet biomass sample will determine two different effects on the pyrolysis process: (i) the decreasing of the reactor temperature due to the drying step, which represents a disadvantage to the pyrolysis process, and (ii) the generated water vapors from moisture content can act like a reactant to improve the intermediate products decomposition (volatile and biochar), which represents an advantage to the pyrolysis process. Which of two effects will play a dominant role depends on the heating rate, but the obtained results demonstrated that under fast pyrolysis conditions the second effect dominated the whole process, whereas the first effect could be neglected. For the slow pyrolysis process, it also can be observed that the CO_2 content shows a decreasing trend with humidity amount from biomass sample increases (Table 2) and this is an interesting behavior, but the interpretation is not very clear, and further study is required. However, the CO_2 decreasing represents a useful parameter for improving the gas quality.

3.3. Effects of Stripping Gas Flow Rate on the Hydrogen Yield

In this study, the stripping gas flow rate was varied from 50 to 0 L/h and the hydrogen yield obtained from walnut shells pyrolysis with various flow rates is presented in Figure 8 and Table 3.

The stripping gas flow rate presents an important effect on the hydrogen yield, this has increased with the decreasing of the stripping gas flow rate. A possible explanation may be that the higher flow rate of stripping gas increased the transport speed of uncondensed volatiles compounds from the reaction zone, decreasing secondary reactions, such as thermal cracking, repolymerization or recondensation [36,39].

In addition, for the direct pyrolysis of the WS_W sample, the higher flow rate of stripping gas also quickly removes the generated water vapors from the reaction zone of the reactor, thus reducing the steam reforming of the intermediate products (volatile and biochar).

Using a lower stripping gas flow (N_2), more intermediate products (volatile and biochar) are transformed into gases, resulting in a higher degree of conversion and a higher amount of gaseous

product. It can be also observed that hydrogen and the CO amount varied with the stripping gas flow rate, while for the rest of gases no important difference was seen.

In Figure 9 is shown the distributions of water and solid fractions for the WS_W sample and its pyrolysis products. The high yield of gas related to the solid fraction contained in WS_W shows that a lot of part of moisture amount reacted with the intermediate compounds (volatile and biochar).

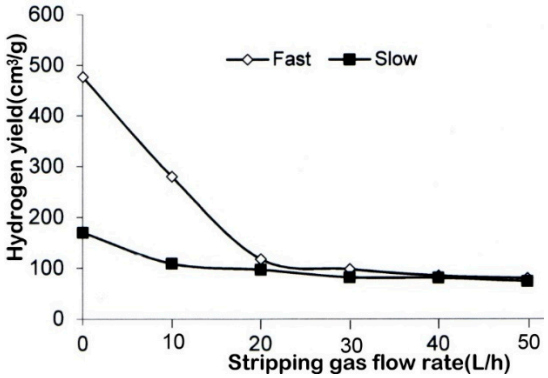

Figure 8. Effect of the stripping gas flow rate on hydrogen yield under different pyrolysis conditions (slow and fast pyrolysis process).

Table 3. The influence of the stripping gas flow rate on the gas yield, conversion efficiency (η) and gas composition.

Parameter	Sample								
	Slow Pyrolysis				Fast Pyrolysis				
	WS_W	WS_W	WS_W	WS_W	WS_W	WS_W	WS_W	WS_W	WS_{TD}
[a] Moisture content (wt.%)	48.15	48.15	48.15	48.15	48.15	48.15	48.15	48.15	7.85
Heating rate (°C/min)	5	5	5	5	50	50	50	50	50
Temperature pyrolysis (°C)	700	700	700	700	700	700	700	700	700
Stripping gas flow rate (L/h)	50	30	10	0	50	30	10	0	0
[b] Gas yield(cm^3/g)	334	411	479	551	539	692	938	1295	901
η (vol.%)	26.76	30.81	36.05	37.12	49.57	60.24	70.06	87.25	68.22
Gas composition (vol.%)									
H_2	26.83	31.17	30.97	38.01	15.78	20.26	31.55	38.06	29.43
CO	36.57	32.77	31.24	24.07	42.35	36.98	26.36	21.43	29.11
CO_2	23.24	22.61	23.30	24.14	31.50	32.04	31.02	30.40	31.38
CH_4	13.36	13.45	14.49	13.78	10.37	10.72	11.07	10.11	10.08

[a] Determined on the wet basis; [b] Determined on the dry ash free basis.

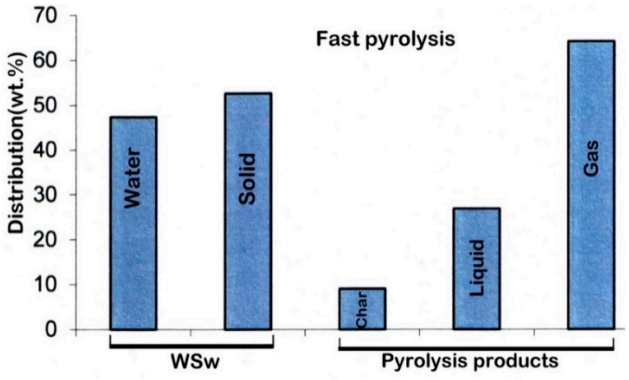

Figure 9. The distribution of water and solid fractions for WS_W and its pyrolysis products. The test was performed under the fast pyrolysis process without N_2 stripping gas.

On the other hand, the fast pyrolysis of the WS_{TD} sample, without stripping gas was also performed and the results are also shown in Table 3. The WS_W pyrolysis released a higher hydrogen yield of 38.06 vol.%, than those of 29.43 vol.%, respectively, from WS_{TD}, indicating a significant increasing of hydrogen yield. The modification of both hydrogen and carbon monoxide contents maybe due to the water gas shift reaction. The higher H_2 content of 38.06 vol.%, obtained in this study, was similar with that was obtained in other studies [7,10] at the same temperature value.

3.4. Biochar Yield and Its Characteristics

In Figure 10 is shown the biochar yield obtained in the slow and fast pyrolysis of WS_W,WS_{PD} and WS_{TD} samples, respectively. It can be seen that the moisture content from samples had also an influence on the biochar yield.

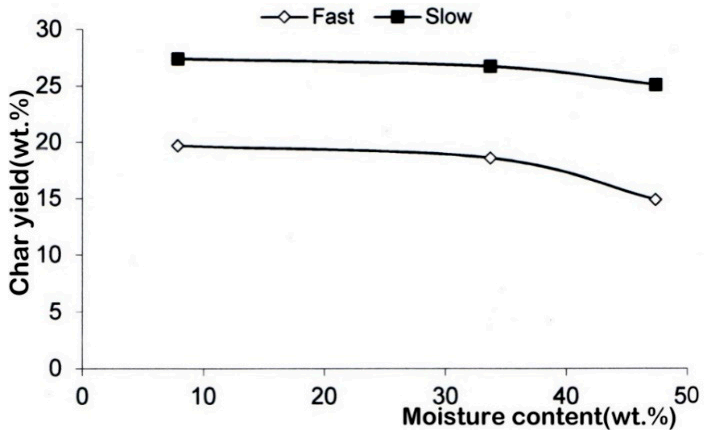

Figure 10. The biochar yield from pyrolysis of WS_W, WS_{PD} and WS_{TD} under slow and fast heating rates.

With the increasing in the moisture content the biochar yield decreased, which is more evidence for the fast pyrolysis process.

This behavior is due to the following reasons: (i) the changing of the internal biomass pores before and after drying step. Using conventional drying methods, raw biomass usually suffers a mass reduction process after drying treatment, which leads to a low gas diffusivity. In our tests, the drying rate, even for the slow pyrolysis process, was faster than those from conventional drying methods. This higher drying rate determined the creation of big channels and much more open pores, even if the structure of the biomass tissue was fragmented, and the release from solid particles of the generated organic molecules was facilitated during the pyrolysis/gasification process; (ii) the nascent char gasification with water vapors was amplified because the increase of the water vapors partial pressure as a result of higher moisture content from biomass samples and (iii) the shorter residence time of volatile products into biomass particles, determined from the improving gas permeability, as above shown, and a fast heating rate, decreased intraparticle volatile cracking and char deposition, the result being a lower biochar yield. The X-ray intensity curves of WS_W sample and CWS_w (char resulted from the WS_W pyrolysis) and CWS_{TD} (char resulted from the WS_{TD} pyrolysis) are given in Figure 11 and SEM images are shown in Figure 12. The pyrolysis tests were carried out under slow heating conditions (slow pyrolysis experiment).

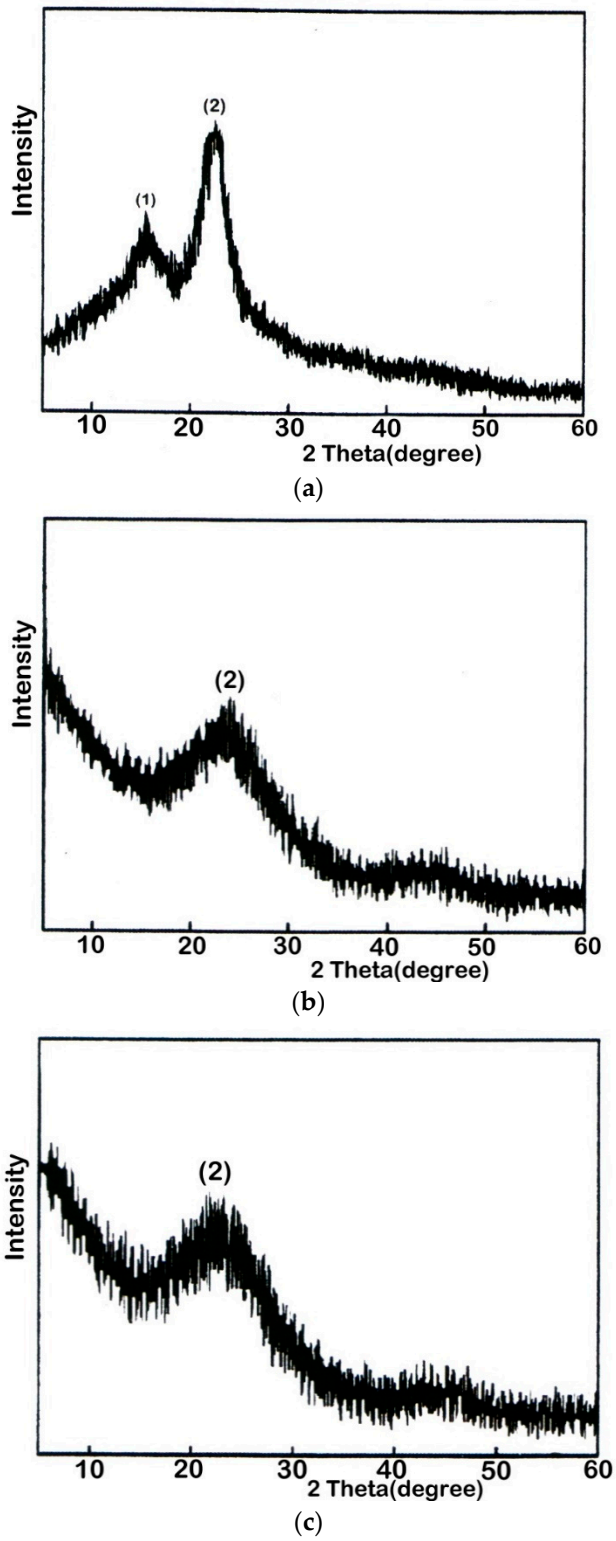

Figure 11. X-ray intensity curves: (**a**) WS_w; (**b**) CWS_w and (**c**) CWS_{TD} (slow heating rate; reactor pyrolysis temperature of 800 °C).

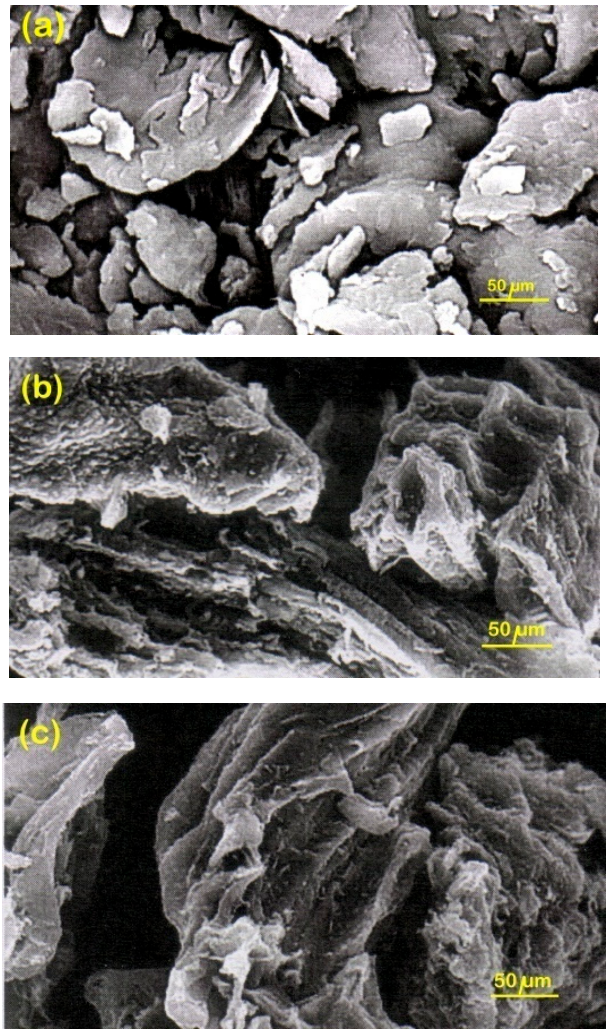

Figure 12. SEM images of: (**a**)—wet walnut shells (WS_w); (**b**)—wet walnut shell-based char (CWS_w) and (**c**)—total dried walnut shell—based char (CWS_{TD}), reactor pyrolysis temperature of 800 °C.

For the WS_W sample, the X-ray intensity curve shows two peaks in low angle 2θ (range 5–36°), and these corresponded to the γ band (1) and to (002) band (2), respectively (see Figure 11a). After pyrolysis of WS_W and WS_{TD} samples, the γ band was not visible, had almost disappeared and the (002) band decreased, as can be seen in Figure 11b,c. The γ band certainly corresponded to aliphatic chains and the (002) band represented the aromatic compounds, this being in agreement with other studies [22,26]. The obtained results show that a lot part of aliphatic chains were decomposed in the pyrolysis process, while only some parts of the aromatic compounds were decomposed. In addition, it also can be seen that the intensity of CWS_W curve was lower than that of CWS_{TD}. This lower intensity curve of CWS_W highlighted that much more aliphatic and aromatic groups were detached from biomass particles for the WS_W pyrolysis than that for the WS_{TD} pyrolysis and this was in agreement with the biochar yield changing, as can be observed in Figure 11. The SEM method was used to analysis the surface physical morphology of the raw walnut shell and biochar obtained after the pyrolysis test. Figure 12a shows the micrograph for the wet walnut shell used as the raw material in the pyrolysis process. The material shows a surface morphology in the form of particles with rough, compact and porous structure. Figure 12b,c shows the micrographs for the biochar obtained after pyrolysis of WS_w and WS_{TD} samples. It can be observed that both biochar samples (CWS_w and CWS_{TD}, respectively) had an approximately smooth surface and different from the rough surface of the raw walnut shell,

but there was not obvious differences in shape and pores structure between the two biochar samples. The biochar yields, elemental analysis, surface area and micropore volume are shown in Table 4.

Table 4. The biochar yields, elemental analysis, surface area and micropore volume for walnut shell pyrolysis at a low heating rate (5 °C/min) and high heating rate (50 °C/min) and moisture content 7.85 wt.% at 800 °C.

Characteristic	Low Heating Rate	High Heating Rate
	(5 °C/min)	**(50 °C/min)**
Char yield (wt.%, dry basis)	31.8	21.6
C	88.15	81.92
H	0.72	1.54
N	0.75	0.56
O	10.38	15.98
H/C	0.0980	0.2255
O/C	0.0883	0.1463
Surface area (m^2/g)	592	536
Micropore volume(cm^3/g)	0.227	0.205

In the pyrolysis process at a temperature below 400 °C, the biochar surface area did not change too much, due to an incomplete removal of volatile compounds from biomass. At a pyrolysis temperature in a range 400–500 °C, the biochar surface area began to increase and the increasing continued up to a pyrolysis temperature at least of 800 °C. This increase could be up to 600 m^2/g. The increasing of the carbon surface area with the increasing of the pyrolysis temperature is due to the formation of the microporous structure [40]. In Table 5 it is shown the effect of pyrolysis temperature on physical properties (surface area and micropore volume) of biochar produced from walnut shells pyrolysis.

Table 5. The temperature effect on the physical properties of the biochar (surface area and micropore volume) for walnut shell pyrolysis at a low heating rate (5 °C/min) and high heating rate (50 °C/min) and moisture content 7.85 wt.%, at 800 °C.

Characteristic	Low Heating Rate				High Heating Rate		
	(5 °C/min)				**(50 °C/min)**		
	500 °C	**600 °C**	**700 °C**	**800 °C**	**600 °C**	**700 °C**	**800 °C**
Surface area (m^2/g)	483	571	587	592	506	521	536
Micropore volume (cm^3/g)	0.167	0.217	0.223	0.227	0.198	0.203	0.205

Additionally, chemical properties of biochar change with biomass type and pyrolysis process conditions, for example, functional groups present in biochar can change by the pyrolysis temperature [40–42]. Usually, the H/C and O/C rates for biomass is about 1.2–1.8 and 0.55–0.75, respectively and this indicates that the biomass has low aromaticity content and has a high aliphatic content [43,44]. For walnut shells the H/C and O/C rates were 1.3105 and 0.6863, respectively (see Table 1). Pyrolysis leads to a significant decreasing in the H/C and O/C atomic ratios, the H/C and O/C rates for resulted biochar were in the range 0.098 to 0.2255 for the low heating rate and 0.0883–0.1463 for the high heating rate, respectively (Table 4).

The changes were more important with the increase of pyrolysis temperature. Below 500 °C, the major reactions were mainly dehydration, decarboxylation and decarbonylation. However, at a temperature above 500 °C, dehydrogenation is the major reaction. These different reactions could affect the characteristics and functionality of the char. This carbon-based material with typical size features in the lower nanometer size range will be attractive for fundamental research and potential new applications, such as for environment applications (sorbent or catalytic material). The results also show the relationships between pyrolysis conditions and product characteristics and the research is

intended to use the biomass residues to produce both hydrogen rich gas with the aim to become an important clean energy resource and biochar with a high porous structure.

4. Conclusions

Residual biomass, such as agricultural residue, represents a valuable renewable energy source and there are different ways by which biomass energy can be transformed into fuels. In this study were used walnut shells as a raw biomass source. Pyrolysis experiments of wet and dry walnut shells were performed and the influence of humidity amount on the hydrogen yield in the gas phase was estimated. The tests were carried out to analyze the influence of the operating parameters (temperature, humidity content, flow rate of the stripping gas and heating rate) on the pyrolysis process and hydrogen yield in gas fraction. The results lead to some conclusions: (i) The pyrolysis of wet walnut shells without the step of predried favored the production of hydrogen-rich gas. Under fast pyrolysis and without the usingofN_2 stripping gas, the pyrolysis of the WS_W sample releases higher H_2 yield than those obtained from the WS_{TD} sample;(ii) In order for the water vapors releasing from its own humidity amount of the walnut shells to be used to obtain more hydrogen, the fast pyrolysis process was required; (iii) The stripping gas flow rate had influence on hydrogen yield, with the decreasing of the stripping gas flow rate the hydrogen yield increased and (iv) This study demonstrated that a new steam supply way is possible by combination of the predrying step with the water vapors generating from wet biomass and thus making this method much more efficient and economical.

At a pyrolysis temperature below 400 °C, the biochar surface area did not change too much, due to an incomplete removal of volatile compounds from biomass, while at a pyrolysis temperature in a range of 400–500 °C, the char surface area began to increase and the increasing continued up to a pyrolysis temperature at least of 800 °C. The increasing of biochar surface area with pyrolysis temperature was due to the development of microporous structure. Pyrolysis led to a significant decreasing in the H/C and O/C atomic ratios, the H/C and O/C rates were in the range 0.098–0.2255 for the biochar resulted by pyrolysis with a low heating rate and 0.0883–0.1463 for biochar resulted by pyrolysis with a high heating rate, respectively.

Funding: This research was funded by the Romanian Ministry of Education and Research under 19N/2019 Financing Contract, NUCLEU Program, Project PN 19 11 03 01/2019-2022—"Studies on the obtaining and improvement of the acido-basic properties of the nanoporous catalytic materials for application in wastes valorization".

Acknowledgments: Iacknowledge the support offered by the Romanian Ministry of Education and Research through19N/2019 Financing Contract, Project PN 19 11 03 01/2019-2022.

Conflicts of Interest: I declare that the research was conducted in the absence of any commercial or financial relationships that could be construed as a potential conflict of interest.

References

1. Hu, X.; Gholizadeh, M. Biomass pyrolysis: A review of the process development and challenges from initial researches up to the commercialization stage. *J. Energy Chem.* **2015**, *39*, 109–143. [CrossRef]
2. Chen, G.; Yao, J.; Liu, J.; Yan, B.; Shan, R. *Biomass* to hydrogen-rich syngas via catalytic steam reforming of bio-oil. *Renew. Energy* **2016**, *91*, 315–322. [CrossRef]
3. Yaman, S. Pyrolysis of biomass to produce fuels and chemical feedstocks. *Energy Convers. Manag.* **2004**, *45*, 651–671. [CrossRef]
4. Demirbas, A. Pyrolysis of Biomass for Fuels and Chemicals. *Energy Sources Part A* **2009**, *31*, 1028–1037. [CrossRef]
5. Liu, Q.; Xiong, Z.; Syed-Hassan, S.S.A.; Deng, Z.; Zhao, X.; Su, S.; Xiang, J.; Wang, Y.; Hu, S. Effect of the pre-reforming by Fe/bio-char catalyst on a two-stage catalytic steam reforming of bio-oil. *Fuel* **2019**, *239*, 282–289. [CrossRef]
6. Chen, J.; Zhao, K.; Zhao, Z.; He, F.; Huang, Z.; Wei, G.; Xia, C. Reaction schemes of barium ferrite in biomass chemical looping gasification for hydrogen-enriched syngas generation via an outer-inner looping redox reaction mechanism. *Energy Convers. Manag.* **2019**, *89*, 81–90. [CrossRef]

7. Demirbas, A. Bio-hydrogen generation from organic wastes. *Energy Sources Part A* **2008**, *30*, 475–485. [CrossRef]
8. Swami, S.M.; Chaudhari, V.; Kim, D.S.; Sim, S.J.; Abraham, M.A. Production of hydrogen from glucose as a biomass simulant: Integrated biological and thermochemical approach. *Ind. Eng. Chem. Res.* **2008**, *47*, 3645–3651. [CrossRef]
9. Hamad, M.; Radwan, A.; Heggo, D.; Moustafa, T. Hydrogen rich gas production from catalytic gasification of biomass. *Renew. Energy* **2016**, *85*, 1290–1300. [CrossRef]
10. Long, Y.D.; Fang, Z.; Su, T.C.; Yang, Q. Co-production of biodiesel and hydrogen from rapeseed and Jatropha oils with sodium silicate and Ni catalysts. *Appl. Energy* **2014**, *113*, 1819–1825. [CrossRef]
11. Balat, H. Prospects of biofuels for a sustainable energy future: A critical assessment. *Energy Educ. Sci. Part A* **2010**, *24*, 85–111.
12. Tyagi, V.K.; Angériz Campoy, R.; Álvarez-Gallego, C.J.; Romero García, L.I. Enhancement in hydrogen production by thermophilic anaerobic co-digestion of organic fraction of municipal solid waste and sewage sludge–optimization of treatment conditions. *Bioresour. Technol.* **2014**, *164*, 408–415. [CrossRef]
13. Parthasarathy, P.; Narayanan, K.S. Hydrogen production from steam gasification of biomass: Influence of process parameters on hydrogen yield—A review. *Renew. Energy* **2014**, *66*, 570–579. [CrossRef]
14. Shahirah, M.N.; Ayodele, B.V.; Gimbun, J.; Cheng, C.K. Samarium promoted Ni/Al_2O_3 catalysts for syngas production from glycerol pyrolysis. *Bull. Chem. React. Eng. Catal.* **2016**, *11*, 238–244. [CrossRef]
15. Kaiwen, L.; Bin, Y.; Tao, Z. Economic analysis of hydrogen production from steam reforming process: A literature review. *Energy Sources Part B Econ. Plan. Policy* **2017**, *13*, 109–115. [CrossRef]
16. Yamakawa, C.K.; Qin, F.; Mussatto, S.I. Advances and opportunities in biomass conversion technologies and biore fi neries for the development of a bio-based economy. *Biomass Bioenergy* **2018**, *119*, 54–60. [CrossRef]
17. Sumrunronnasak, S.; Tantayanon, S.; Kiatgamolchai, S.; Sukonket, T. Improved hydrogen production from dry reforming reaction using a catalytic packed-bed membrane reactor with Ni-based catalyst and dense PdAgCu alloy membrane. *Int. J. Hydrogen Energy* **2016**, *41*, 2621–2630. [CrossRef]
18. Ghimire, A.; Trably, E.; Frunzo, L.; Pirozzi, F.; Lens PN, L.; Esposito, G.; Cazier, E.A.; Escudié, R. Effect of total solids content on biohydrogen production and lactic acid accumulation during dark fermentation of organic waste biomass. *Bioresour. Technol.* **2018**, *248*, 180–186. [CrossRef]
19. Arregi, A.; Amutio, M.; Lopez, G.; Bilbao, J.; Olazar, M. Evaluation of thermochemical routes for hydrogen production from biomass: A review. *Energy Convers. Manag.* **2018**, *165*, 696–719. [CrossRef]
20. Salam, M.A.; Ahmed, K.; Akter, N.; Hossain, T.; Abdullah, B. A review of hydrogen production via biomass gasification and its prospect in Bangladesh. *Int. J. Hydrogen Energy* **2018**, *43*, 14944–14973. [CrossRef]
21. Luo, M.; Yi, Y.; Wang, S.; Wang, Z.; Du, M.; Pan, J.; Wang, Q. Review of hydrogen production using chemical-looping technology. *Renew. Sustain. Energy Rev.* **2018**, *81*, 3186–3214. [CrossRef]
22. Feng, Y.; Luo, S.; Hu, Z.; Xiao, B.; Cheng, G. Hydrogen-rich gas production by steam gasification of char from biomass fast pyrolysis in a fixed-bed reactor: Influence of temperature and steam on hydrogen yield and syngas composition. *Bioresour. Technol.* **2010**, *101*, 5633–5637.
23. Balat, M. Mechanisms of thermochemical biomass conversion processes. Part 2: Reactions of gasification. *Energy Sources Part A* **2008**, *30*, 636–648.
24. Soria, J.; Li, R.; Flamant, G.; Mazza, G.D. Influence of pellet size on product yields and syngas composition during solar-driven high temperature fast pyrolysis of biomass. *J. Anal. Appl. Pyrolysis* **2019**, *140*, 299–311. [CrossRef]
25. Balat, M. Possible methods for hydrogen production. *Energy Sources Part A* **2009**, *31*, 39–50. [CrossRef]
26. Wang, Y.; Jiang, L.; Hu, S.; Su, S.; Zhou, Y.; Xiang, J.; Zhang, S.; Li, C.Z. Evolution of structure and activity of char-supported iron catalysts prepared for steam reforming of bio-oil. *Fuel Process. Technol.* **2017**, *158*, 180–190. [CrossRef]
27. Yoon, S.J.; Choi, Y.C.; Lee, J.G. Hydrogen production from biomass tar by catalytic steam reforming. *Energy Convers. Manag.* **2010**, *51*, 42–47. [CrossRef]
28. Jiang, L.; Lin, Q.; Lin, Y.; Xu, F.; Zhang, X.; Zhao, Z.; Li, H. Impact of ball-milling and ionic liquid pretreatments on pyrolysis kinetics and behaviors of crystalline cellulose. *Bioresour. Technol.* **2020**, *305*, 123044. [CrossRef]
29. Efika, C.E.; Wu, C.; Williams, P.T. Syngas production from pyrolysis–catalytic steam reforming of waste biomass in a continuous screw kiln reactor. *J. Anal. Appl. Pyrolysis* **2012**, *95*, 87–94. [CrossRef]

30. Ma, Z.; Zhang, S.P.; Xie, D.Y.; Yan, Y.J. A novel integrated process for hydrogen production from biomass. *Int. J. Hydrogen Energy* **2014**, *39*, 274–279. [CrossRef]
31. Dupont, C.; Boissonnet, G.; Seiler, J.M.; Gauthier, P.; Schweich, D. Study about the kinetic processes of biomass steam gasification. *Fuel* **2007**, *86*, 32–40. [CrossRef]
32. Ni, M.; Dennis, Y.C.L.; Michael, K.H.L.; Sumathy, K. An overview of hydrogen production from biomass. *Fuel Process. Technol.* **2006**, *87*, 461–472. [CrossRef]
33. Lv, P.M.; Chang, J.; Xiong, Z.H.; Huang, H.T.; Wu, C.Z.; Chen, Y.; Zhu, J.X. Biomass Air-Steam Gasification in a Fluidized Bed to Produce Hydrogen-Rich Gas. *Energy Fuels* **2003**, *17*, 677–682. [CrossRef]
34. Chaudhari, S.T.; Dalai, A.K.; Bakhshi, N.N. Production of hydrogen and/or syngas (H_2 + CO) via steam gasification of biomass-derived chars. *Energy Fuels* **2003**, *17*, 1062–1067. [CrossRef]
35. Domınguez, A.; Menendez, J.A.; Pis, J.J. Hydrogen rich fuel gas production from the pyrolysis of wet sewage sludge at high temperature. *J. Anal. Appl. Pyrolysis* **2006**, *77*, 127–132. [CrossRef]
36. Mahishi, M.R.; Goswami, D.Y. An experimental study of hydrogen production by gasification of biomass in presence of a CO_2 sorbent. *Int. J. Hydrogen Energy* **2007**, *32*, 2803–2808. [CrossRef]
37. Pűtűn, A.E.; Apaydın, E.; Pűtűn, E. Bio-oil production from pyrolysis and steam pyrolysis of soybean-cake: Product yields and composition. *Energy* **2002**, *27*, 703–713. [CrossRef]
38. Apaydi-Varol, E.; Pűtűn, E.; Pűtűn, A.E. Slow pyrolysis of pistachio shell. *Fuel* **2007**, *86*, 1892–1899. [CrossRef]
39. Tsai, W.T.; Lee, M.K.; Chang, Y.M. Fast pyrolysis of rice straw, sugarcane bagasse and coconut shell in an induction-heating reactor. *J. Anal. Appl.* **2006**, *76*, 230–237. [CrossRef]
40. Liu, W.-J.; Zeng, F.-X.; Jiang, H.; Zhang, X.-S. Preparation of high adsorption capacity bio-chars from waste biomass. *Bioresour. Technol.* **2011**, *102*, 8247–8252. [CrossRef]
41. Ahmad, M.; SooLee, S.; Dou, X.; Mohan, D.; Sung, J.-K.; Yang, J.E.; SikOk, Y. Effects of pyrolysis temperature on soybean stover- and peanut shell-derived biochar properties and TCE adsorption in water. *Bioresour. Technol.* **2012**, *118*, 536–544. [CrossRef]
42. Balat, M.; Kırtay, E.; Balat, H. Main routes for the thermo-conversion of biomass into fuels and chemicals. Part 2: Gasification systems. *Energy Convers. Manag.* **2009**, *50*, 3158–3168. [CrossRef]
43. Demirbas, M.F. Biorefineries for biofuel upgrading: A critical review. *Appl. Energy* **2009**, *86*, 151–161. [CrossRef]
44. Demirbas, A.H. Biofuels for future transportation necessity. *Energy Educ. Sci. Technol. Part A* **2010**, *26*, 13–23.